

THE EFFECT OF STITCH REMOVAL ON FORMING-INDUCED DEFECTS FOR NON-CRIMP FABRICS

A. M. Joesbury*, S. Chen, L. Cadinouche, N. A. Warrior, L.T. Harper
Composites Research Group, University of Nottingham, Nottingham, United Kingdom

* Corresponding author (adam.joesbury@nottingham.ac.uk)

Keywords: NCF, preform, forming, stitch removal, defects, metrology

ABSTRACT

The dry fibre reinforcement format of Non-Crimp Fabric (NCF) is used preferentially over woven fabrics when very high structural stiffness is required for liquid moulded composites, as the fibres are not interlaced and tend to remain straight. Production parts are not typically planar and therefore require forming to produce curved geometries from these broad good fabrics. NCF materials are therefore prone to forming defects, due to their high in-plane shear stiffness and high out-of-plane bending stiffness compared to woven textiles. Previous work has demonstrated that selectively removing stitches from NCF can improve formed part quality by eliminating out-of-plane wrinkling defects. This paper focuses on categorising in-plane defects that occur when a pillar stitched biaxial NCF is formed by positive and negative shear, identifying defect types including ‘in-plane fibre waviness’, ‘kink bands’, and ‘slip lines’. It is found that removal of stitches can result in the additional defect types of ‘unrestrained fibre bundle waviness’, ‘loose fibres’ and ‘laddering’.

Two distinct metrology methods are studied to determine the effect of stitch removal on the local fibre orientations over the surface of formed components. A Hexagon AB APODIUS Vision System is compared with a low-cost optical reflectance method, which both yield comparable results in terms of identifying the in-plane fibre angles. Finally, the next step in the overall study is laid-out, this being to characterise the in-plane defect types in terms of fibre architecture topology and mechanical characteristics so that defect severity can be understood. This information can then be used, together with the mapping of defect locations, to update parameters for a future iteration of the genetic-algorithm used to optimise the stitch-removal pattern.

1 INTRODUCTION

Forming processes are an essential step in producing low-cost, high-volume composites for both the automotive and aerospace sectors. Fabrics, UD fibres, or even sheet moulding compounds must be rapidly converted from 2D blanks into complex 3D forms. This study further explores a new method of controlling textile deformation during automated forming processes to achieve higher quality fabric preforms.

Non-Crimp Fabric (NCF) is a dry fabric format that is used to produce composite structures requiring high stiffness and strength. The fabric consists of layers of continuous unidirectional fibres that are held together by through-thickness stitching. Multiple fibre layers at various fibre directions can constitute a fabric, which is particularly desirable when high-rate deposition is an important manufacturing consideration. The stitch yarns provide stability to the fabric, avoiding unwanted distortion during material handling and layup. Consequently, the inherent stiffness of NCF materials can lead to challenges when forming high curvature geometries. Additionally, the stitch lines have been found to be capable of carrying significant load, which can introduce forming asymmetry and early onset of in-plane fabric shear locking. These stitch-influenced characteristics can result in fibre architecture defects, such as out-of-plane ply folds or wrinkles and in-plane fibre waviness.

Methods such as using additional stitching [1] or local injection of resin [2] have been studied to improve preform quality. Recently published work has investigated whether modifying as-received

fabrics by localised discrete removal of stitches can also be used as a technique to mitigate the occurrence of out-of-plane ply folds. A genetic-algorithm was developed to automatically generate an optimised stitch-removal pattern, removing a total of 30% of the stitches across the blank area, which successfully eliminated out-of-plane ply folds for a punch-formed biaxial NCF [3]. A follow-on study has identified that while stitch removal can be beneficial in controlling out-of-plane defects, excessive removal of stitches can increase the likelihood of in-plane defects. The present work builds on this finding by systematically investigating the effect of local stitch removal on in-plane defect types that occur when biaxial NCF fabrics are formed.

2 OVERVIEW AND SCOPE

Ongoing work is investigating how finite element simulation can be used in conjunction with genetic algorithms to produce optimised forming processes. The methodology reported here is to modify the material properties of the NCF blanks by selectively removing inter-ply stitches from discrete areas prior to forming, with the aim of improving the quality of the formed part. Figure 1 shows a flowchart of the physical process steps and corresponding digital data that when generated informs the optimisation algorithm.

Stage 1 [3] used data acquired from a Coordinate Measuring Machine (CMM), qualitative visual inspection, and fabric shear properties, to set limits within a genetic algorithm-based optimisation protocol to remove local stitches and eliminate out-of-plane wrinkling. The current paper focuses on Stage 2, which aims to categorise and quantify other types of fibre architecture defects that are generated during the forming process, as a result of the stitch removal process. These defects typically include various forms of in-plane fibre wrinkling that are less obvious to identify compared to out-of-plane wrinkling. Qualitative visual inspection of formed parts enables defects within the fibre architecture to be identified and categorised, however the routine use of such labour-intensive methods is economically unfeasible. Therefore, the use of novel metrology methods is investigated to acquire data accurately and repeatedly. The planned Stage 3 of the project will investigate the criticality of defects in terms of the detrimental effect on mechanical performance. Outcomes from Stages 2 and 3 will be combined to provide an extended set of limitations to be used in a second iteration of the genetic algorithm optimisation protocol.

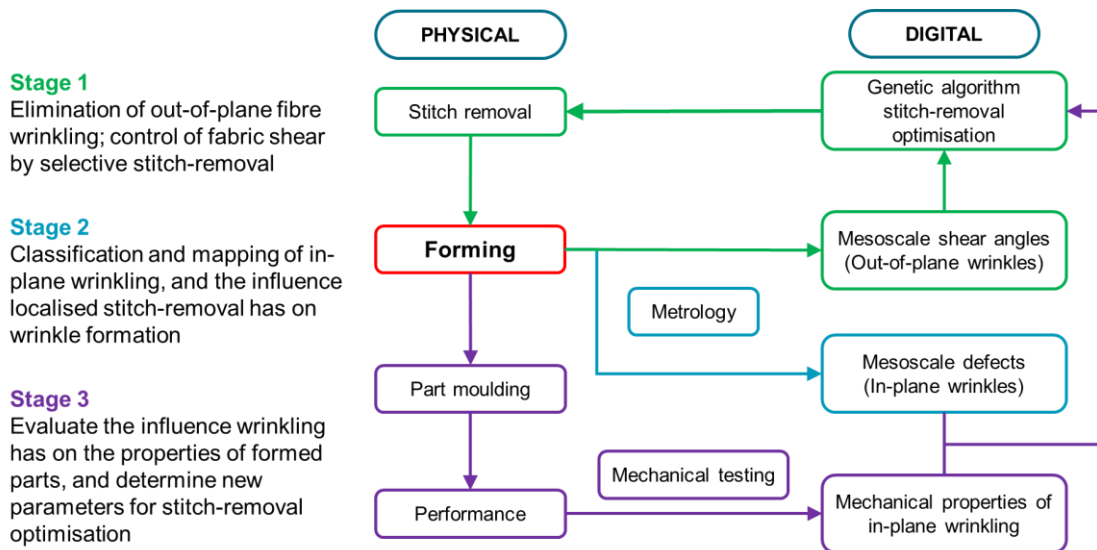


Figure 1: Diagram showing the physical process steps of producing formed parts together with digitised information that can be used in optimisation protocols to intelligently modify material properties prior to processing.

3 MATERIALS AND METHODS

A laboratory-scale hemisphere forming tool was used for preforming the NCF, which was integrated within a universal testing machine (Instron 5581) using the method outlined in [4] and illustrated in Figure 2. Two 300 mm × 300 mm heated square platens with central holes (104 mm diameter) were used as blank holders to clamp the fabric plies. A small amount (6% wt) of reactive binder (Momentive Epikote 05390) was applied to the surface of the ply, in order to create a stiff preform for post-forming analysis. A clamping force of 1200 N was applied to the blank holder. A hemispherical punch with a diameter of 100 mm was attached to the crosshead of the machine via a 50 kN load cell, which allowed the forming force to be monitored. A punch speed of 100 mm/min was used to form the plies. Each forming experiment was performed at ambient temperature, before the temperature of the hemispherical punch and square platens was ramped to 165 °C and held for 10 min to cure the binder. Experiments were conducted using punch displacements of 50 mm (causing the hemisphere to become fully formed).

Biaxial NCF blanks (FCIM359) with dimensions 300 x 300 mm square were prepared with the 0° and 90° fibre directions aligned with the blank edges and the 45° stitch direction aligned diagonally across the blank. Full-scale stencils of the stitch removal patterns were used to manually plot the patterns onto the fabric blanks. Stitches were removed using a soldering iron to melt-sever stitches at each point of intersection between the stitch line and the plotted pattern. Each stitch line was then completely removed by unravelling the stitch chain, removing all stitching material with minimum disruption to the fibre architecture. Figure 3 (d) shows the quality of the stitch removal area achieved by this method.

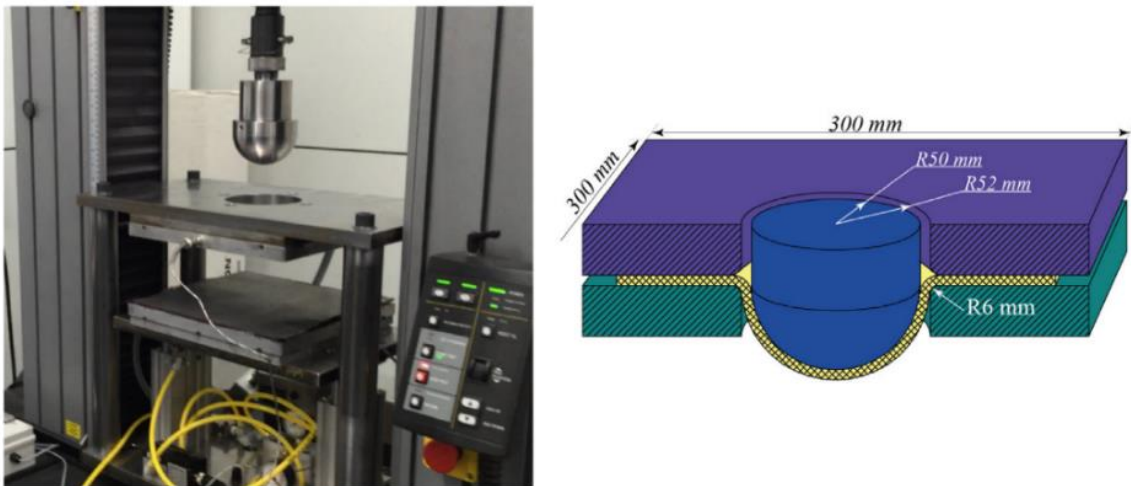


Figure 2: Laboratory-scale hemisphere forming, (a) tool installed on universal testing machine and (b) diagram of formed part within closed tool, reproduced from Chen et al [4].

Fabric blanks with stitches removed were created for two patterns: a ‘defect-informed’ pattern and an optimised pattern according to the genetic algorithm in [3]. The defect-informed pattern was chosen to investigate how defect formation is affected by stitch removal. The pattern was derived by removing stitches from areas that were identified from baseline formed parts, which had no stitches removed, and so exhibit significant amounts of in-plane or out-of-plane wrinkling. Figure 3 illustrates the areas identified for the defect-informed stitch removal pattern. The optimised stitch-removed pattern from the genetic algorithm [3] is shown in Figure 3 (f). Both patterns removed the same total amount of stitches, which was 30% of the total area.

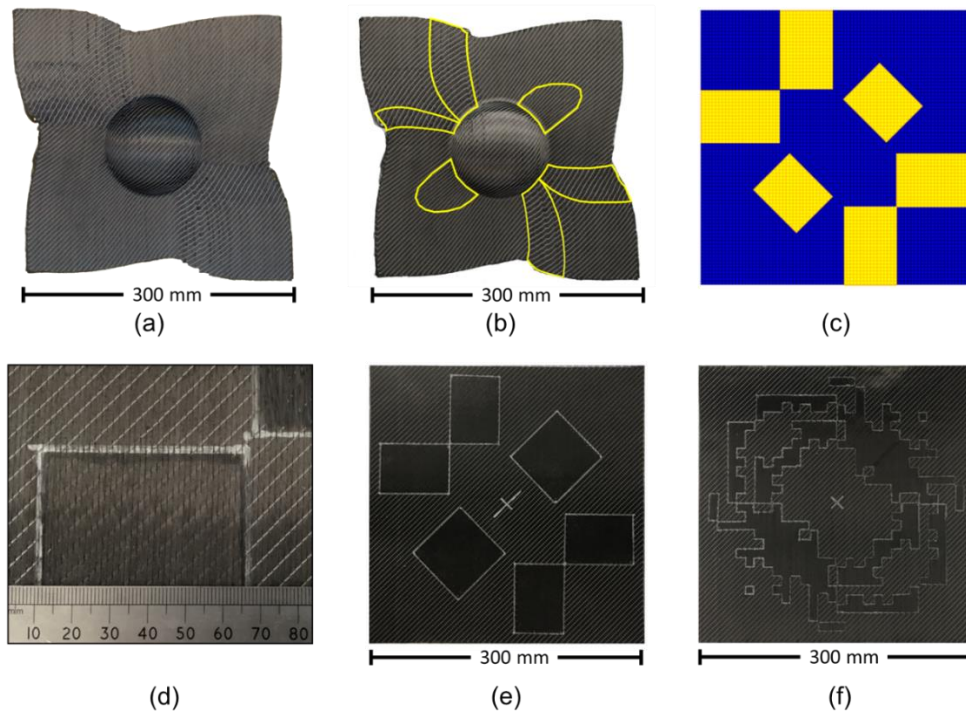


Figure 3: Derivation of ‘defect-informed’ intuitive stitch removal pattern; (a) baseline formed specimen, (b) areas of defect identified, (c) stitch removal areas based on defect locations, (d) area showing stitch removal; stitches removed with minimum disruption to the underlying fibre architecture, (e) blank with stitches removed, (f) for comparison the optimised stitch-removal pattern.

Two metrology methods were used to measure fibre angles on the formed parts. The first method used the Hexagon AB APODIUS Vision System, which is a commercially available turnkey system that acquires and processes photographic images to identify fibre orientation using propriety software and hardware. The second method was developed by Pierce et al [5] and exploits the reflectivity of carbon fibre to identify fibre orientation. This method is relatively low cost, being implementable with a generic light source and photographic apparatus to acquire images, which are subsequently processed by a MATLAB script written in line with the published methodology.

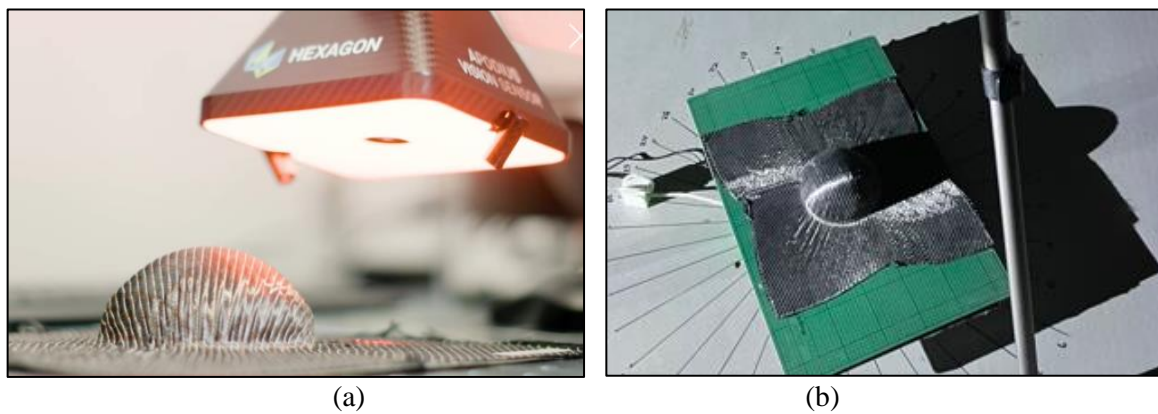


Figure 4: Metrology methods used in this study were (a) the Hexagon AB APODIUS Vision System and (b) the optical carbon fibre reflectance orientation analysis method developed by Pierce et al [5].

4 RESULTS

The regions of major in-plane shear are identified in Figure 5 [4], which indicates that the greatest positive and negative shear angles occur around the hemisphere perimeter and extend away from the centre in diverging directions. This divergence can clearly be seen in the pattern of defects in the negative shear regions in Figure 6 (a) and (b). The divergence of positive shear is more diffuse with defects occurring in only one region: Figure 6 (c). The formed parts have an approximate rotational symmetry of 180° , therefore it is considered that there are three distinct regions where forming defects occur, which are repeated twice due to the rotational symmetry. The two negative shear regions are denoted as Zones 1 and 2, and the single positive region is denoted as Zone 3.

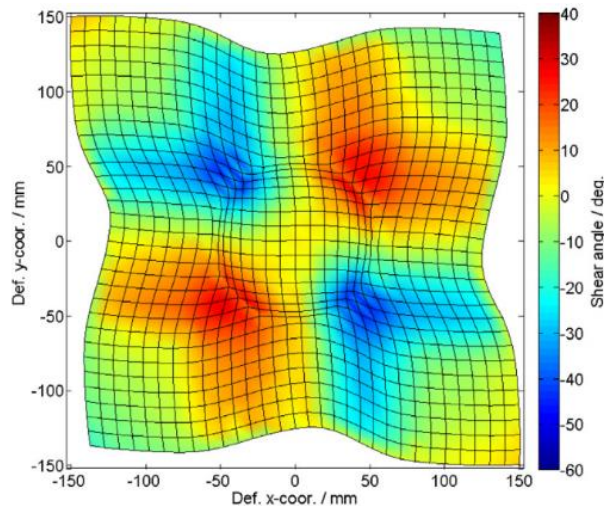


Figure 5: Measured fabric shear as a result of hemisphere punch forming. Red regions indicate positive shear (stitch lines in tension) and blue regions indicate negative shear (stitch lines in compression). Figure reproduced from Chen et al [4].

Visual inspection of the formed parts enabled identification of sub-categories of in-plane defects. Direct comparison was then made with corresponding areas on formed parts where stitches had been removed prior to forming. A summary of these effects is presented in Table 1, including a subjective assessment on the relative quality of the fibre architecture topology.

Defects that occur in the baseline hemispheres are categorised as either inter-stitch bundle waviness, kink bands or slip lines. Inter-stitch bundle waviness occurs predominantly when compressive forces are applied along the length of the fibres, due to regions of positive shear. The points where stitch interlacings penetrate fibre layers act to restrain in-plane fibre architecture deformations, effectively controlling the frequency of wrinkles. Figure 6 (c) shows an example of inter-stitch fibre bundle waviness in the positive shear region. Inter-stitch bundle waviness also occurs when stitch lines are compressed and this will be discussed later in this section.

Kink bands occur in regions of negative shear, as fibres abruptly change angle due to shear deformation. This is a mesoscale analogy to the microscale kink band defect phenomenon that can occur when reinforcement fibres of a composite material locally deform by micro-buckling due to globally applied compression. An example of a kink band can be seen in Figure 6 (b). Inter-stitch fibre bundle waviness can also be observed in the area between the kink bands. The wavelength of inter-stitch waviness is longer in the negative shear regions compared to the positive shear regions, as the spacing between stitch lines is greater in these areas.

Slip lines occur in regions of negative shear, when the shear deformation causes groups of fibres to slip excessively past one another. This defect type can be seen in Figure 6 (a). The NCF fabric used in this study is biaxial, therefore a relationship exists between the defects observed on each outer surface of the ply in regions of negative fabric shear. When kink bands with inter-stitch waviness is present on one surface of the fabric then slip lines are present on the opposing fabric surface, and vice-versa.

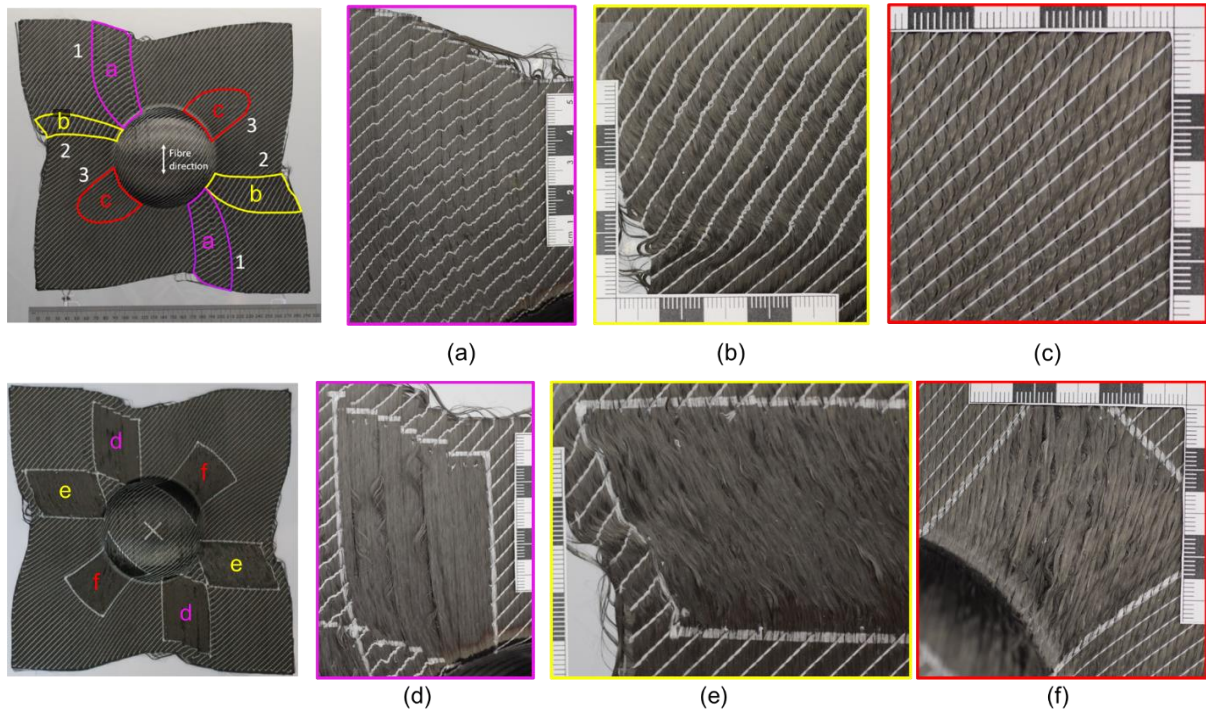


Figure 6: (Top row) In-plane defects for a preform containing all stitches (a), (b), (c). (Bottom row) In-plane defects for a preform where local stitches have been removed prior to forming (d), (e), (f).

Inspection of formed parts where stitches had been removed reveals the presence of alternative fibre defects, which can be categorised as unrestrained bundle waviness, loose fibres, and laddering. Figure 6 (e) and (f) show examples of unrestrained bundle waviness, which tends to occur in areas similar to those that exhibited inter-stitch fibre bundle waviness when stitches had not been removed. Loose fibres are present in areas that are prone to the slip line defect, as shown in Figure 6 (d). Loose fibres occur at the boundary of slip lines due to fibres being dragged out of position because of inter-fibre friction from the relative motion of fibre groups moving past each other. Loose fibres occur due to the loss of fibre constraints that results from the absence of stitches.

An additional defect that is a result of stitch removal is laddering, which is shown in Figure 7. Laddering was first observed to a limited extent when the genetic algorithm optimised stitch removal pattern was trialed, Figure 7 (a). An additional specimen was made with a larger area of removed stitches, Figure 7 (b), which revealed an increased propensity for laddering. Laddering occurs because of a combination of lack of fibre constraint, due to the absence of stitches, in conjunction with the forming draw-in motion being transverse to the fibre direction.

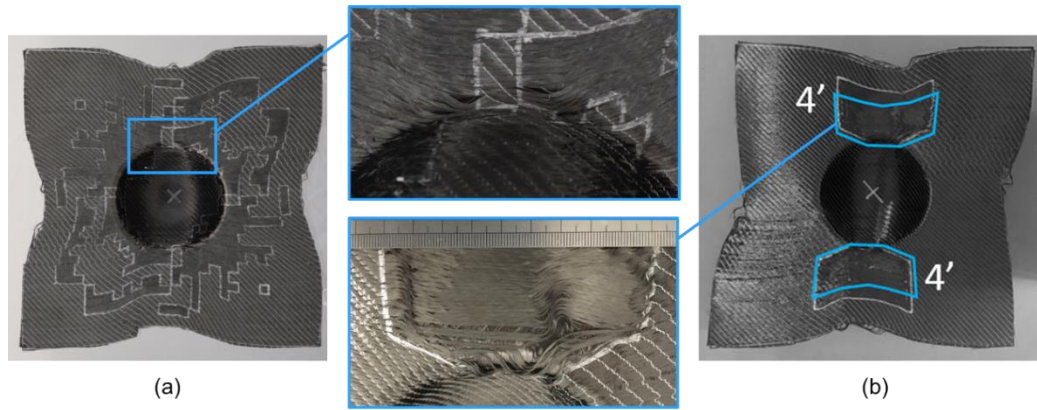


Figure 7: Laddering defect, (a) seen to a limited extent with the genetic algorithm optimized stitch removal pattern, (b) and with greater severity when larger continuous areas of stitches are removed.

Shear state	Images	Defects in baseline	Defects when stitches removed	Effect on fibre architecture quality
Positive	<i>Figure 6 (c)</i> <i>Figure 6 (f)</i>	Out-of-plane wrinkles, Inter-stitch bundle waviness	Unrestrained fibre bundle waviness	Improvement
Negative	<i>Figure 6 (a)</i> <i>Figure 6 (d)</i>	Slip lines	Slip lines, Loose fibres	Deterioration
Negative	<i>Figure 6 (b)</i> <i>Figure 6 (e)</i>	Kink band, Inter-stitch bundle waviness	Kink band, Unrestrained fibre bundle waviness	Neutral
Neutral	<i>Figure 7 (a)</i> <i>Figure 7 (b)</i>	None	Laddering	Deterioration

Table 1: Summary of the effect stitch removal has on defects.

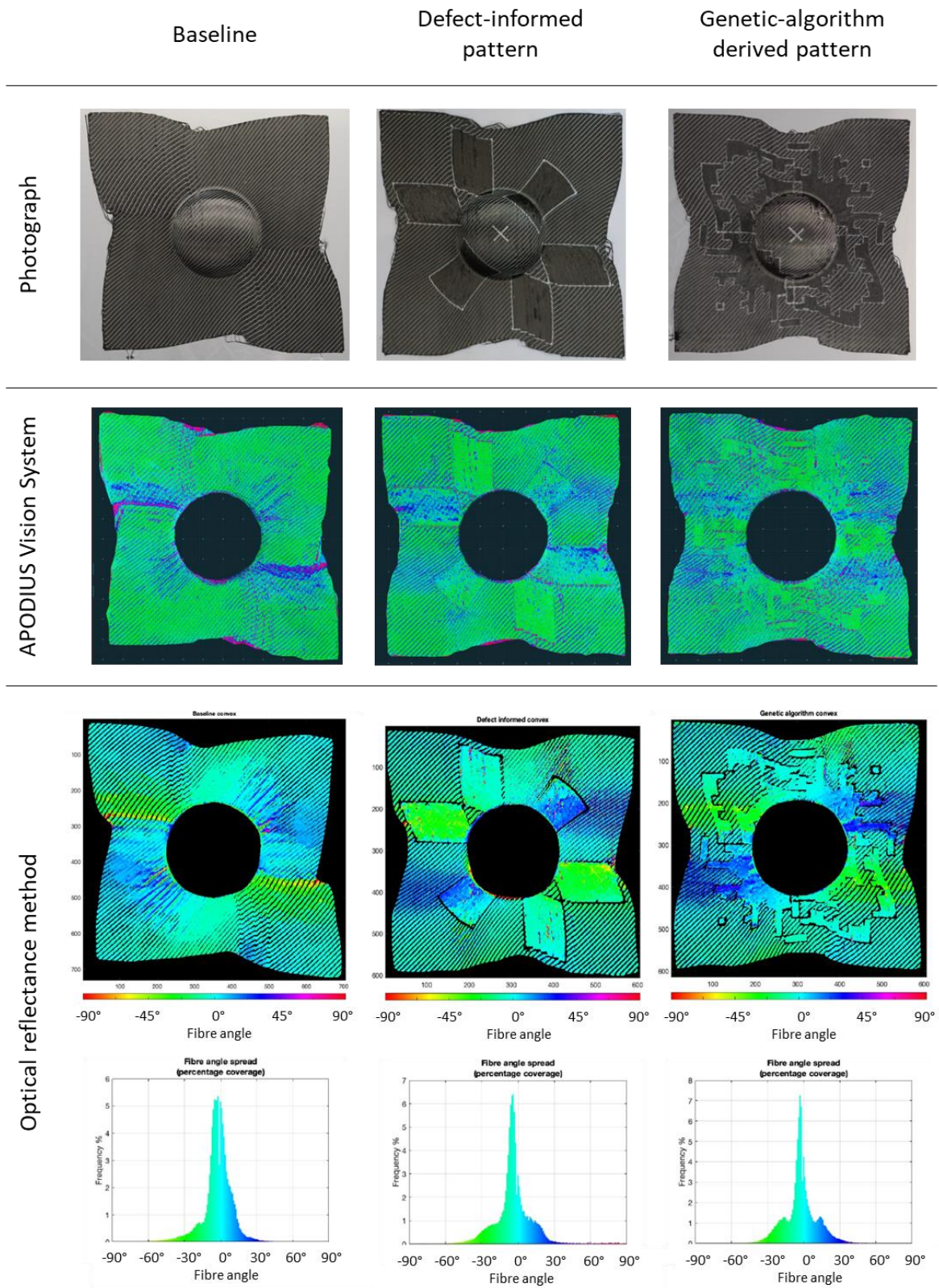


Figure 8: Comparison of scan results of formed parts, (1st row) reference photographs of formed parts, (2nd row) output scans of APODIUS Vision System, (3rd row) results from optical reflectance method, (4th row) fibre angle spread from optical reflectance method. All rows are of the same three formed parts, from left to right: no stitch removed baseline, defect informed stitch-removal pattern, optimised stitch removal pattern.

Results from the metrology scans show that there is a comparable level of detail between the APODIUS Vision System, Figure 8 (2nd row), and the optical reflectance method, Figure 8 (3rd row). The fibre orientation contour produced by the APODIUS Vision System is coloured green for 0° fibres, with other colours representing fibre angle deviation away from 0°. There is no differentiation between positive or negative fibre angles. The orientation plot from the optical reflectance method shows cyan for 0° fibres with colours tending towards blue for positive fibre angles and green for negative fibre angles.

From the results of both scanning methods, as shown in Figure 8, fibre angle deviation is strongly localised in the baseline formed part (no stitches removed). The fibre angle deviation is less localised for the defect-informed stitch-removal pattern, extending to adjacent regions compared to the baseline formed part, with this effect being greater still for the optimised stitch removal pattern. However, as can be seen in Figure 9, there are areas where the optimised stitch removal pattern results in significantly localised fibre angle deviation compared to the defect informed stitch-removal pattern.

When compared to the defects identified in *Figure 6*, regions where out-of-plane wrinkles, inter-stitch bundle waviness, and kink bands occur can clearly be seen in the scans for the baseline formed part. However, the scanning methods used in this study produce global fibre angle heatmaps of the entire parts and, as can be seen in the detail views of Figure 9, defect types cannot be directly identified from the scan results. Areas where slip line defects occur cannot be directly observed from scans, however discontinuities of stitch lines indicate the presence of this defect type. Loose fibres can be directly observed from both scan types.

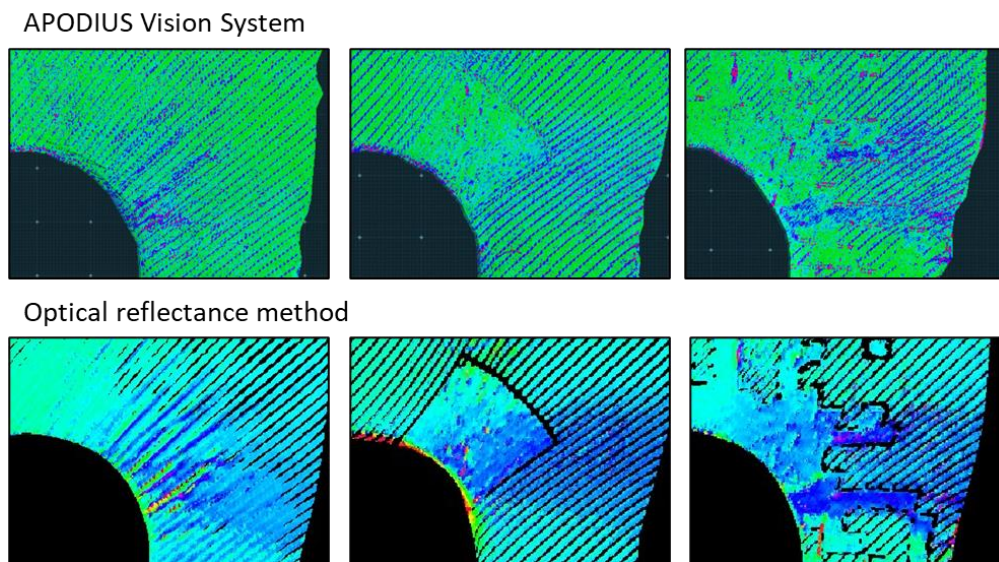


Figure 9: Detail views of scanning results of formed parts for comparison of the two methods. All images are of the positive region of the formed specimens, which are (from left to right) no stitches removed, defect informed stitch-removal pattern, and optimised stitch-removal pattern.

5 CONCLUSIONS

In baseline formed parts, which have no stitches removed, three distinct types of in-plane fibre architecture defects are identified. These defects are inter-stitch bundle waviness, kink bands, and slip lines. The type of in-plane defect corresponds to fabric shear state and are dependent on the fabric fibre direction and the relative direction of NCF stitch lines.

Removal of stitches has been previously demonstrated to eliminate out-of-plane wrinkling, but excessive removal of stitches can have a detrimental effect on the appearance of in-plane defects. It is therefore suggested that stitch removal should be minimized in locations prone to these defects.

Two metrology methods have been demonstrated to be capable of mapping and quantifying the local in-plane fibre orientation state. The low-cost fibre reflectance method is demonstrated to have equivalent capabilities to more expensive vision-based systems; however, the fibre reflectance method is currently limited to 2D surfaces. Where fibre architecture defects do not result in fibre angle deviation, for example slip lines, the defect type cannot be directly observed, however discontinuities of stitch line paths are observable and can therefore be used to indirectly identify these defects.

6 FUTURE WORK

Further work is required to understand whether the metrology systems trialled in this study can identify defect types when mapping the global distribution of fibre angles for a formed part. This would include further postprocessing of scan data and use of image acquisition equipment with higher resolution capabilities.

The next step of this work, as outlined by ‘Stage 3’ in Figure 1, will be to characterise the properties of in-plane fibre architecture defects. This will include topological measurements of fibre waviness and mechanical testing of moulded laminates that contain induced representative defects. The measured properties will enable an understanding of the severity of defect types and will be used to define updated parameters for a future iteration of the optimised stitch-removal pattern genetic-algorithm protocol [3] to produce new optimisation patterns that account for both out-of-plane and in-plane defect types.

ACKNOWLEDGEMENTS

This work was funded by the Engineering and Physical Science Research Council [Grant number: EP/P006701/1], as part of the “EPSRC Future Composites Manufacturing Research Hub”. Access to the APODIUS system was kindly provided by the HV-Command EPSRC Strategic Equipment Grant (EP/T006420/1) at the University of Nottingham.

REFERENCES

- [1] S. Chen, A. Endruweit, L. T. Harper, and N. A. Warrior, “Inter-ply stitching optimisation of highly drapeable multi-ply preforms,” *Compos. Part A Appl. Sci. Manuf.*, vol. 71, pp. 144–156, 2015.
- [2] M. A. Turk, B. Vermes, A. J. Thompson, J. P. H. Belnoue, S. R. Hallett, and D. S. Ivanov, “Mitigating forming defects by local modification of dry preforms,” *Compos. Part A Appl. Sci. Manuf.*, vol. 128, no. July 2019, p. 105643, 2020.
- [3] S. Chen, A. M. Joesbury, F. Yu, L. T. Harper, and N. A. Warrior, “Optimisation of intra-ply stitch removal for improved formability of biaxial non-crimp fabrics,” *Compos. Part B Eng.*, vol. 229, no. November 2021, 2022.
- [4] S. Chen, O. P. L. McGregor, L. T. Harper, A. Endruweit, and N. A. Warrior, “Defect formation during preforming of a bi-axial non-crimp fabric with a pillar stitch pattern,” *Compos. Part A Appl. Sci. Manuf.*, vol. 91, pp. 156–167, 2016.
- [5] R. S. Pierce and X. Liu, “Exploiting the optical reflectance behaviour of carbon fibre composites for low-cost inspection and orientations analysis,” *J. Reinf. Plast. Compos.*, vol. 39, no. 23–24, pp. 869–879, 2020.